

# Corneal polarimetry after LASIK refractive surgery

Juan M. Bueno

Esther Berrio

Pablo Artal

Universidad de Murcia  
Laboratorio de Óptica  
Campus de Espinardo (Edificio C)  
30071, Murcia, Spain

**Abstract.** Imaging polarimetry provides spatially resolved information on the polarization properties of a system. In the case of the living human eye, polarization could be related to the corneal biomechanical properties, which vary from the normal state as a result of surgery or pathologies. We have used an aberro-polariscope, which we recently developed, to determine and to compare the spatially resolved maps of polarization parameters across the pupil between normal healthy and post-LASIK eyes. The depolarization distribution is not uniform across the pupil, with post-surgery eyes presenting larger levels of depolarization. While retardation increases along the radius in normal eyes, this pattern becomes irregular after LASIK refractive surgery. The maps of slow axis also differ in normal and post-surgery eyes, with a larger disorder in post-LASIK eyes. Since these changes in polarization indicate subtle structural modifications of the cornea, this approach can be useful in a clinical environment to follow the biomechanical and optical changes of the cornea after refractive surgery or for the early diagnosis of different corneal pathologies. © 2006 Society of Photo-Optical Instrumentation Engineers. [DOI: 10.1117/1.2154747]

Keywords: polarimetry; LASIK; depolarization; retardation; corneal axis.

Paper 05159R received Jun. 29, 2005; revised manuscript received Sep. 5, 2005; accepted for publication Sep. 7, 2005; published online Jan. 24, 2006.

## 1 Introduction

During the last decade, laser *in situ* keratomileusis (LASIK) has become a widely used technique for the correction of ocular ametropias.<sup>1</sup> Although it has been proven successful in eliminating with reasonable precision defocus and astigmatism, standard LASIK affects visual performance. Several studies evaluated the influence of LASIK on visual acuity and contrast sensitivity<sup>2-4</sup> and investigated the changes in the eye's aberrations after the surgery.<sup>5</sup>

In addition to the induced aberrations, corneal haze<sup>6-8</sup> is one of the most important possible negative effects of this surgery. Nowadays the mechanisms that produce this haze are still unclear. Other related issues such as the biomechanical response of the cornea to the ablation and the wound-healing process are also under investigation.<sup>9,10</sup>

The stroma removal<sup>11</sup> during surgery and the cutting and folding-back of the flap<sup>12,13</sup> change the physical and biomechanical properties of the cornea (thickness, curvature, scattering processes, stress, etc.). On the other hand, the polarization properties of any system are known to be directly associated with its structure.<sup>14</sup> Despite the fact that the eye has complicated polarization properties (see, for instance, Ref. 15 as a general review), birefringence of the cornea is the main contributor to the polarization properties in a normal eye.

In this context, we propose the measurement of ocular (or alternatively corneal) polarization properties to be used to test changes in the structural and biomechanical properties of the after-LASIK eyes. Along with this work we compare spatially

resolved polarization properties in young normal and post-LASIK eyes. These results will permit better understanding of the possible changes produced by LASIK refractive surgery in the structural properties of the cornea and their potential impact in vision.

## 2 Methods

### 2.1 Apparatus and Experimental Procedure

We used an aberro-polariscope instrument, recently developed in our laboratory.<sup>16</sup> It combines a Hartmann-Shack (HS) wavefront sensor and a polarimeter. The system simultaneously measures the eye's wavefront aberrations (WA) and spatially resolved polarization properties. Figure 1 shows a schematic diagram of the experimental apparatus.

A collimated infrared laser beam (780-nm wavelength and 1.5 mm in diameter) vertically polarized (by use of P1) enters the eye. After reflection in the retina, the outgoing beam passes a focus corrector (FC) system and the analyzer unit [AU; consisting of a quarter-wave plate ( $\lambda/4$ ) that can be orientated appropriately and a vertical linear polarizer (P2)]. Finally, the beam is sampled by the array of microlenses (ML; 45-mm focal length and 0.6-mm aperture), conjugated with the eye's pupil and focused on a cooled scientific-grade CCD camera. The FC consists of a pair of achromatic doublets (L1 and L2, 190- and 200-mm focal lengths, respectively) separated by three mirrors, two of them (M2 and M3) placed on a translation stage. The head of the subject was stabilized with a bite-bar mounted on a three-axis positioning stage. An additional video camera (not shown in the figure) monitors the position of the subject's pupil during the experiment.

Address all correspondence to Juan Bueno, Laboratorio de Óptica, Universidad de Murcia, Campus de Espinardo (Edificio C), Murcia, Murcia 30071, Spain. Tel: 34-969398335. Fax: 34-968363528. E-mail: bueno@um.es

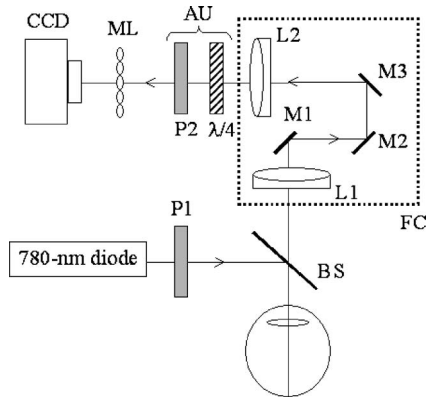


**Fig. 1** Simplified schematic diagram of the aberropolariscope.  $M_1$ – $M_3$ , mirrors; ML, microlens array; BS, beam splitter. Further details are provided in the text.

Measurements were carried out in the eyes of two groups of subjects with ages ranging from 25 to 40 years. The first group was composed of 4 eyes (2 LE and 2 RE) from 4 normal healthy subjects and they were used as a control group. These subjects did not present a prior history of ocular pathologies and they had a corrected visual acuity of 20/20 or better. The second group included 4 eyes (2 LE, 2 RE) from two post-LASIK patients that underwent a successful standard LASIK surgery (VISX STAR S2™). Individual pre-surgery refractions for LASIK eyes were  $(-6.50)(-0.50)10^\circ$ ,  $(-5.75)(-1.00)0^\circ$ ,  $(-5.00)(-3.50)30^\circ$ , and  $(-4.75)(-2.75)155^\circ$ . Post-surgery averaged refraction was  $-0.125 \pm 0.125D$ . The control eyes presented low amounts of astigmatism, with refractions  $-1.5$ ,  $(+0.50)(-0.50)20^\circ$ ,  $-2.25$ , and  $(-1.00)(-0.25)90^\circ D$ . The ablation area was 6 mm in diameter. The measurements were obtained with natural pupil diameter and at least one month after the surgery.

A series of four, 2-s exposure, HS images corresponding to independent polarization states in AU were recorded. These different polarization states were obtained by placing the fast axis of the  $\lambda/4$  plate at four different angles<sup>17</sup>:  $-45$ ,  $0$ ,  $30$ , and  $60^\circ$ . The WA aberration was calculated from each individual HS image as described elsewhere.<sup>18</sup> For each set of four HS images, the Stokes vector ( $\mathbf{S}_{\text{OUT}}$ ) associated with the polarization state of light emerging from the eye was reconstructed for each spot in the HS image. The spatial resolution of the polarimetric measurements is limited by the area of each microlens on the pupil plane.  $\mathbf{S}_{\text{OUT}}$  is calculated by:

$$\mathbf{S}_{\text{OUT}} = \begin{pmatrix} S_0 \\ S_1 \\ S_2 \\ S_3 \end{pmatrix} = (\mathbf{M}_{\text{PSA}})^{-1} \begin{pmatrix} I_1 \\ I_2 \\ I_3 \\ I_4 \end{pmatrix} \quad (1)$$

where  $\mathbf{M}_{\text{PSA}}$  is an auxiliary matrix<sup>17</sup> and  $I_i$  ( $i=1, 2, 3, 4$ ) are the averaged intensity of each spot for the four HS images. The degree of polarization (DOP), the retardation ( $\delta$ ), and the azimuth of the slow axis ( $\alpha$ ), associated with corneal birefringence, were computed from the Stokes vector by using:

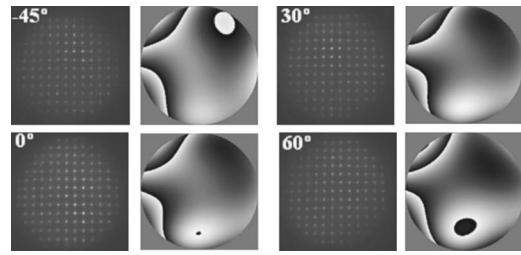


**Fig. 2** HS images and associated WA maps for each independent polarization state in the AU for a normal eye of the control group.

$$\text{DOP} = \frac{\sqrt{S_1^2 + S_2^2 + S_3^2}}{S_0}, \quad (2)$$

$$\alpha = \frac{1}{2} a \tan\left(-\frac{\text{DOP} + S_1}{S_2}\right) + 90^\circ, \quad (3)$$

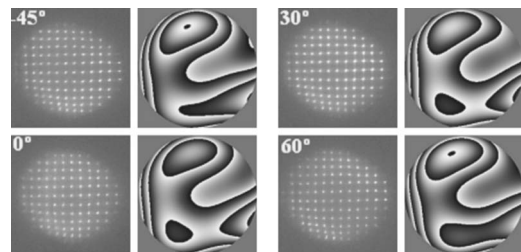
$$\delta = a \cos\left(1 + \frac{2S_2}{\text{DOP} \cdot \sin(4\alpha)}\right). \quad (4)$$

Throughout this paper the term “depolarization” will refer to the 1-DOP.

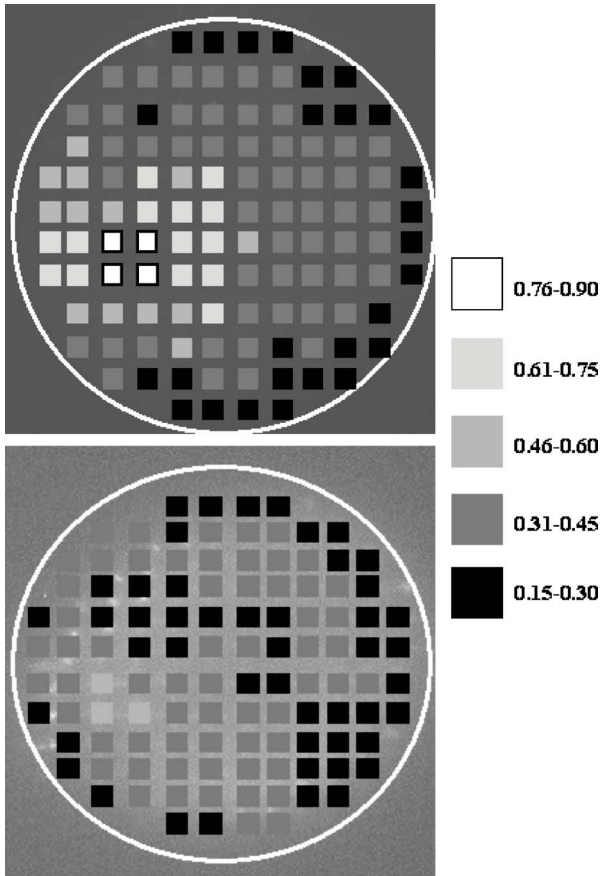
### 3 Results

Figure 2 presents an example of the HS images for the four polarization states, together with the corresponding WA maps in one of the control eyes. Figure 3 shows the same results for a post-LASIK eye. As is well known, the aberrations in the post-LASIK eyes are higher than in normal eyes. On the other hand, in both types of eyes, the WAs were similar for the four independent polarization states. In particular, for the case of Fig. 2, the root-mean-square (RMS) values of the WA for a 5-mm pupil were  $0.26 \pm 0.05$ ,  $0.29 \pm 0.05$ ,  $0.33 \pm 0.03$ , and  $0.32 \pm 0.01 \mu\text{m}$  for the  $-45$ -,  $0$ -,  $30$ -, and  $60$ -deg polarizations, respectively. The RMS values (also for a 5-mm pupil) for the case of Fig. 3 were  $0.55 \pm 0.03$ ,  $0.54 \pm 0.04$ ,  $0.59 \pm 0.06$ , and  $0.58 \pm 0.03 \mu\text{m}$ .

In the following figures, we will show a comparison of the spatially resolved corneal polarization properties between post-LASIK and control eyes. Figure 4 shows the spatially resolved DOP for both a control and a post-LASIK eye. The position of the pupil of the eye is shown by a white circle ( $\sim 6$  mm in diameter). This size is similar for all subsequent figures. The DOP is not uniform across the pupil, presenting a



**Fig. 3** HS images and associated WA maps for each independent polarization state in the AU for a post-LASIK eye.



**Fig. 4** Spatially resolved DOP for two right eyes for a normal (upper panel) and a post-LASIK (bottom panel) eye. The gray scale is shown on the right. The white circle indicates the position of the eye's pupil (~6 mm in diameter).

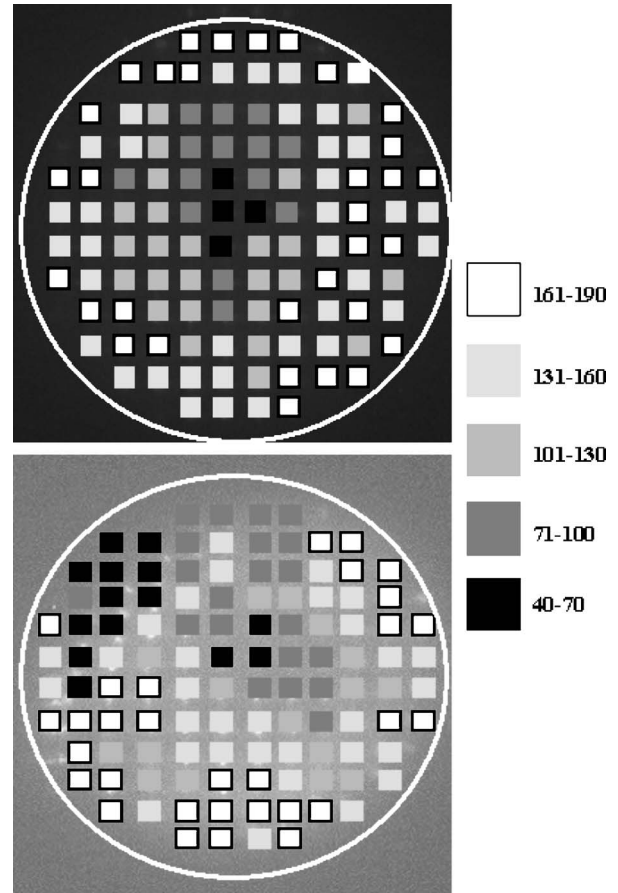


**Fig. 5** Distribution (spot by spot) of corneal retardation in the right eye of a normal (upper panel) and a post-LASIK (bottom panel) eye. Units are degrees.

maximum (with a location that is dependent on each subject and usually is not exactly centered) and it decreases toward the edges of the pupil. While the lower values of DOP are similar in both eyes, the maximum values are higher in the control normal eye than in the post-LASIK eye. Table 1 shows the averaged maximum and minimum DOP values across the pupil for both groups of subjects. Standard deviations (for all series and analyzed spots) were similar for both types of eyes and ranged from 0.04 to 0.11.

Figure 5 shows the maps of corneal retardation for both a control and a post-LASIK eye. For the normal healthy eye, the retardation is lowest in the center and increases toward the margins of the pupil (retardation is gray-scale-coded in the figure, with black and white indicating the lower and higher retardation values). In the normal eye of the figure, there is an increase of 124 deg in a radius of 3.2 mm. Central corneal

retardation ranged from 30 to 63 deg. However, the normal pattern of retardation appears to be completely disrupted in the post-LASIK eye. The values of retardation were irregular across the pupil, and low retardation values can even be found near the edge of the pupil. For these eyes the minimum retardation ranged between 16 and 49 deg. Values for the standard deviation for all subjects and series were in the range 6–10 deg without significant differences in repeatability between control and post-LASIK eyes.

Figure 6 shows the distribution of the slow corneal axis (corneal azimuth) in the two eyes: normal and post-LASIK. In the control eye (upper panel) the central azimuth is clearly oriented in the nasal-downward direction, with an average orientation of  $-14 \pm 7^\circ$  for a central area of 2.5 mm in diameter. This is the common behavior in all the normal control eyes, with the azimuths ranging from  $-22^\circ$  to  $11^\circ$  in the central area. Negative and positive values corresponded to right and left eyes, respectively. In the peripheral areas of the pupil, the slow axis rotates with respect to the central orientation: in some areas the orientation is radial while in others it tends to be tangential. In the case of the post-LASIK eye, on average the slow axis in the central part of the pupil is also oriented nasally downward ( $\sim 12^\circ$ , bottom panel in Fig. 6), however, the distribution of the local axis is more disordered than in the control eye, especially toward the periphery of the pupil,

**Table 1** Averaged maximum and minimum DOP values across the pupil for the two groups of eyes.

	DOP max	DOP min
Control	$0.83 \pm 0.12$	$0.18 \pm 0.04$
Post-LASIK	$0.54 \pm 0.02$	$0.17 \pm 0.08$

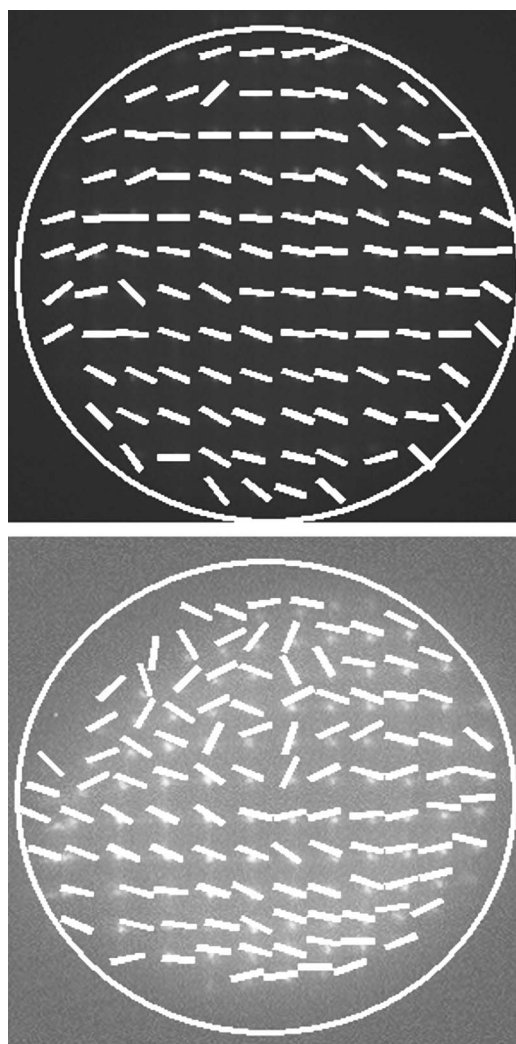


**Fig. 6** Orientation of the corneal slow axis (corneal azimuth) in the same eyes as in previous figure.

where more irregular patterns were found. Variations within different series resulted in standard deviations that were never larger than  $6^\circ$  for both types of eyes.

In order to better show the spatial changes of azimuth across the pupil, Fig. 7 presents the difference between the local azimuth for each location and that of the central area. The map of differences of the control eye (upper panel) is more uniform than that of the post-LASIK eye. In the former the differences are lower at the center and larger at the periphery. However, the distribution is not symmetric around the center. Larger differences can be found near the center in the post-LASIK eye. In addition, the range of differences is clearly larger in this eye, probably as a direct result of the changes induced by surgery. Figure 8 shows the average distribution of differences in azimuth (in %) for all the eyes in both groups. In both types of eyes, the largest percentage corresponds to differences in azimuth smaller than  $17^\circ$ . However in the interval  $[37, 55]$  deg of differences in azimuth the number of locations is noticeably larger in post-LASIK eyes (16%) than in the control group (5%).

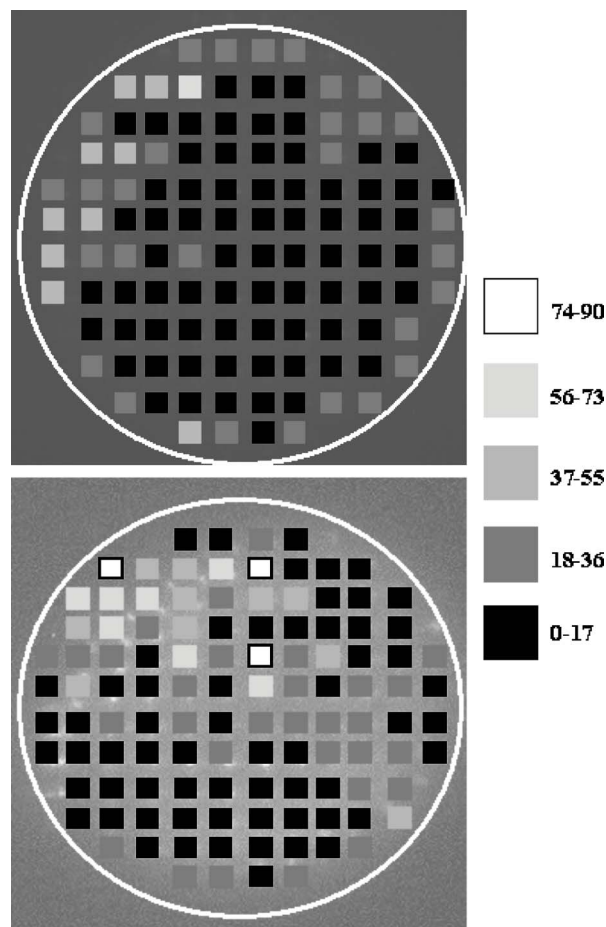


**Fig. 7** Spatially resolved differences (in absolute value) between each local corneal azimuth and that of the central cornea in the same subjects as in previous figures. Units are degrees.

#### 4 Discussion

We have used a new instrument that we designed and built (aberror-polariscope) to measure the spatially resolved polarization parameters in two groups of eyes: one of normal, used as a reference, and a group of post-LASIK eyes. The instrument allowed for the simultaneous measurements of both the eye's WA and spatially resolved polarization properties. Due to its actual physical characteristic (large size, bite bar, etc.),

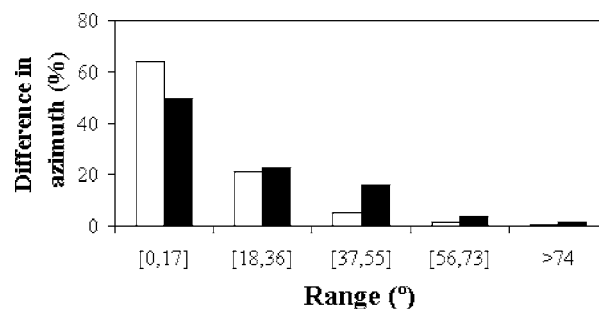


**Fig. 8** Average distribution (in %) of differences between the local corneal azimuths across the pupil and the central one in both control (white bars) and post-LASIK eyes (black bars).



at this moment the system is intended to be used just for basic research. Additional changes are required to be used in a clinical environment for statistical purposes and with nonexperimental subjects. To avoid artifacts in the final polarimetric parameters for both groups of eyes, the intensity of all spots used in the analysis were well above the background of the HS image.

Although the aim of this paper is not the analysis of changes in the WA with refractive surgery, for the sake of completeness, we have also presented HS images and WA maps for both a control and a post-LASIK eye. As expected, eyes that underwent standard LASIK refractive surgery were more aberrated than normal eyes. We demonstrated that the aberrations do not depend on the polarization state of the light neither in control nor in post-LASIK eyes. This agrees well with previous experiments in normal healthy eyes by using different techniques.<sup>19–21</sup>

We compared the spatially resolved polarization parameters such as the DOP, and the retardation and the slow axis associated with corneal birefringence, in normal control and post-LASIK eyes. Although this is not a clinical study and we present a small number of subjects, the differences we found in the two groups might be related with the changes induced by the surgery in the corneal properties. This is a limitation, but results show noticeable differences between these two groups of eyes. Future studies with larger sets of eyes and under different experimental conditions (different amounts of myopia, age, time after surgery, etc.) would help to fully understand, describe, and complete the results presented here.

The DOP at the pupil plane decreases toward the margins, however the maximum is not necessarily located at the center of the pupil. This indicates that apart from the corneal and retinal birefringence there are noticeable depolarization effects, which depend on the area of the pupil analyzed. Overall we have found that the maximum DOP for the control group is 54% higher than the value corresponding to the post-LASIK eyes.

Since the subjects used in this study presented normal retinas and lenses,<sup>22,23</sup> the decrease in the DOP would have its origin in the cornea. Although further measurements are necessary, this decrease in DOP may indicate an increase of corneal haze due to corneal reshaping and wound healing, which reduces the visual acuity and produces glare and mild fogging during the first few months.

Previous studies have shown a nonuniform distribution for the DOP of the light at the pupil's plane using Mueller-matrix polarimetry.<sup>22,24</sup> Van Blokland and van Norren<sup>22</sup> measured the DOP along a horizontal meridian of the pupil plane (3-mm radius) for the light double-passing the ocular media. In general, they found that near the margins of the pupil the parameter is 10% lower than in the central part (0.75). Bueno<sup>22</sup> reported a decrease in the DOP of around 25% in a radius of approximately 2 mm. In the present study the reduction in DOP for the control group was about 22%, but it increased to 31% for the group of post-LASIK eyes. The averaged DOP for the whole pupil was 0.49 and 0.37 for control and post-LASIK eyes, respectively.

The distribution of corneal retardation in normal eyes reveals an increase from the center to the periphery of the pupil with a radial symmetry. However the values depended on each particular eye. For the eyes studied here, retardation

ranged from a minimum of 30° in the center to a maximum of 179° (in a radius of 3 mm). The minimum central retardation has been classically attributed to the perpendicular incidence of the incoming light beam on the corneal surface.<sup>25</sup> On the other hand, the increase of retardation toward the periphery could be due to three reasons: (a) a nonperpendicular incidence, (b) an increase in the corneal thickness, and (c) an increase in the corneal birefringence. Previous experiments with a reduced number of eyes agreed well with these results.<sup>26,27</sup> Spatially resolved studies of *in vivo* corneas have also reported a large variability among subjects, but for most of them the corneal retardation is approximately constant at the central area and increases with the radius.<sup>27,28</sup> Recently Götzinger and co-workers have carried out measurements of corneal birefringent properties using polarization-sensitive optical coherence tomography (PS-OCT).<sup>29</sup> Their results indicate that the retardation increases in a radial direction and with depth.

On the other hand, when observing the map for retardation in post-LASIK eyes, the normal pattern is disrupted and the symmetry in the increment toward the edges of the pupil disappears. Since the experimental conditions are similar for both types of eyes, these changes are thought to be a result of the structural changes in the cornea induced by refractive surgery. Corneal retardation carries out information on thickness and local disturbances in the structure. In this sense, ablation eliminates a fraction of the stroma and this not only modifies the thickness and curvature of the cornea but also its internal structure. This structure is changed in a noncontrolled way, which might induce variations in the birefringence and alternatively in the retardation, which would be associated to a regular pattern. By means of a scanning laser polarimeter with a variable corneal compensator, changes in central corneal retardation before and after LASIK have also been found with ablation.<sup>30</sup> These were thought to be related to the loss of corneal tissue during the process of ablation. Using PS-OCT, an irregular distribution of corneal retardation has also been reported in corneas with keratoconus and scars.<sup>31</sup>

Spatially resolved maps of slow corneal axis also differed between control and post-LASIK eyes. In the former the corneal axis corresponding to the central area is oriented along the upper-temporal to lower-nasal direction. Most axes are parallel to each other and have the same direction in that area. Although the rather uniform tendency of the central corneal axis is well accepted, there are some discrepancies on the distribution outside this area. Our data show that when going toward the periphery the axis rotates and changes its direction. These changes are more pronounced in areas near the edge of the pupil; they are not symmetric around the center. Similar results were reported by van Blokland and Verhelst.<sup>32</sup> In the case of post-LASIK eyes, the spatial distribution of corneal slow axis is not as clear as that observed in control eyes. Despite the nasally-downward central orientation (with higher dispersion), the differences between contiguous areas are much larger in this type of eyes. In fact the number of areas with a difference in axis higher than 35° with respect to the central orientation is always larger in post-LASIK eyes (black bars in Fig. 8). The corneal axis informs on the distribution of the corneal stroma and the directions of stress or tensions. The axis map is altered after corneal ablation, with the local resultant direction of the lamellae changes producing a more

irregular axis pattern in the post-LASIK eyes than in the control eyes.

In summary, we have used an aberro-polariscope to compare the spatially resolved polarization properties between normal and post-LASIK eyes. The latter present larger levels of depolarization and more irregular patterns of retardation and corneal slow axis, which are attributed to the structural changes produced by the ablation process. The patterns of birefringence of control eyes might be used as standards for comparisons with pathological changes. This is the first step in exploring the physical and biomechanical changes produced by refractive surgery using polarization. Additional measurements will be necessary for a better understanding of the post-LASIK changes as a function of the amount of ametropia or the time after surgery. In particular, this technique could be also used in pathological corneas (i.e., keratoconus), in eyes undergoing corneal transplantation or even in the corneal wound repair after surgery.

### Acknowledgments

This research was supported by "Ministerio de Educacion y Ciencia," Spain; Grant Nos. BFM2001-0391 and FIS2004-02153. Dr. José M. Marín performed the LASIK surgery and all the ophthalmic tests in the patients involved in this work.

### References

1. S. Farah, D. Azar, C. Gurdal, and J. Wong, "Laser *in situ* keratomileusis: Literature review of a developing technique," *J. Cataract Refractive Surg.* **24**, 989–1006 (1998).
2. J. T. Holladay, D. R. Dudeja, and J. Chang, "Functional vision and corneal changes after laser *in situ* keratomileusis determined by contrast sensitivity, glare testing, and corneal topography," *J. Cataract Refractive Surg.* **25**, 663–669 (1999).
3. K. Nakamura, H. Bissen-Miyajima, I. Toda, and K. Tsubota, "Effect of laser *in situ* keratomileusis correction on contrast visual acuity," *J. Cataract Refractive Surg.* **27**, 357–361 (2001).
4. Y. K. Nio, N. M. Jansonijs, R. H. Wijdh, W. H. Beekhuis, J. G. Worst, S. Norrby, and A. C. Kooijman, "Effect of methods of myopia correction on visual acuity, contrast sensitivity, and depth of focus," *J. Cataract Refractive Surg.* **29**, 2082–2095 (2003).
5. E. Moreno-Barriuso, J. Merayo-Llodes, S. Marcos, R. Navarro, L. Llorente, and S. Barbero, "Ocular aberrations before and after myopic corneal refractive surgery: LASIK-induced changes measured with laser ray tracing," *Invest. Ophthalmol. Visual Sci.* **42**, 1396–1403 (2001).
6. S. W. Chang, A. Benson, and D. T. Azar, "Corneal light scattering with stromal reformation after laser *in situ* keratomileusis," *J. Cataract Refractive Surg.* **24**, 1064–1069 (1998).
7. J. A. del Val, S. Barrero, B. Yáñez, J. Merayo, J. A. Aparicio, V. R. González, J. C. Pastorm, and S. Mar, "Experimental measurement of corneal haze after excimer laser keratectomy," *Appl. Opt.* **40**, 1727–1734 (2001).
8. J. Bühren and T. Kohnen, "Stromal haze after laser *in situ* keratomileusis: Clinical and confocal microscopy findings," *J. Cataract Refractive Surg.* **29**, 1718–1726 (2003).
9. C. Roberts, "The cornea is not a piece of plastic," *J. Refract. Surg.* **16**, 407–413 (2000).
10. C. K. Park and J. H. Kim, "Comparison of wound healing after photorefractive keratectomy and laser *in situ* keratomileusis," *J. Cataract Refractive Surg.* **25**, 842–850 (1999).
11. W. J. Dupps, Jr. and C. Roberts, "Effect of acute biomechanical changes on corneal curvature after photokeratectomy," *J. Refract. Surg.* **17**, 658–669 (2001).
12. J. Porter, S. MacRae, G. Yoon, C. Roberts, I. G. Cox, and D. R. Williams, "Separate effects of the microkeratome incision and laser ablation on the eye's wave aberration," *Am. J. Ophthalmol.* **136**, 327–337 (2003).
13. S. Waheed, M. R. Chalita, M. Xu, and R. R. Krueger, "Flap-induced and laser-induced ocular aberrations in a two-step LASIK procedure," *J. Refract. Surg.* **21**, 346–352 (2005).
14. M. Born and E. Wolf, *Principles of Optics*, 7th ed., Pergamon Press, New York (1999).
15. L. J. Bour, "Polarized light and the eye," Chap. 13 in *Vision Optics and Instrumentation*, Vol. 1, W. N. Charman, Ed., pp. 310–325, Macmillan Press, London (1991).
16. J. M. Bueno, E. Berrio, and P. Artal, "Aberro-polariscope for the human eye," *Opt. Lett.* **28**, 1209–1211 (2003).
17. J. M. Bueno and J. W. Jaronksi, "Spatially resolved polarization properties for *in vitro* corneas," *Ophthalmic Physiol. Opt.* **21**, 384–392 (2001).
18. P. M. Prieto, F. Vargas-Martin, S. Goelz, and P. Artal, "Analysis of the performance of the Hartmann-Shack sensor in the human eye," *J. Opt. Soc. Am. A* **17**, 1388–1398 (2000).
19. J. M. Bueno and P. Artal, "Polarization and retinal image quality estimates in the human eye," *J. Opt. Soc. Am. A* **18**, 489–496 (2001).
20. P. M. Prieto, F. Vargas-Martin, J. S. McLellan, and S. A. Burns, "Effect of the polarization on ocular wave aberration measurements," *J. Opt. Soc. Am. A* **19**, 809–814 (2002).
21. S. Marcos, L. Díaz-Santana, L. Llorente, and J. C. Dainty, "Ocular aberrations with laser ray tracing and Shack-Hartmann: Does polarization play a role?" *J. Opt. Soc. Am. A* **19**, 1063–1072 (2002).
22. J. M. Bueno, "Depolarization effects in the human eye," *Vision Res.* **41**, 2687–2696 (2001).
23. J. M. Bueno and M. C. W. Campbell, "Polarization properties for *in vitro* old human crystalline lens," *Ophthalmic Physiol. Opt.* **23**, 109–118 (2003).
24. G. J. van Blokland and D. van Norren, "Intensity and polarization of light scattered at small angles from the human fovea," *Vision Res.* **26**, 485–494 (1986).
25. R. W. Knighton and X. -R. Huang, "Linear birefringence of the central human cornea," *Invest. Ophthalmol. Visual Sci.* **43**, 82–86 (2002).
26. B. Pelz, C. Weschenmoser, S. Goelz, J. P. Fischer, R. O. W. Burk, and J. F. Bille, "In vivo measurement of the retinal birefringence with regard on corneal effects using an electro-optical ellipsometer," *Proc. SPIE* **2930**, 92–101 (1996).
27. L. J. Bour and N. J. Lopes Cardozo, "On the birefringence of the living human eye," *Vision Res.* **21**, 1413–1421 (1981).
28. J. M. Bueno and F. Vargas-Martín, "Measurements of the corneal birefringence with a liquid-crystal imaging polariscope," *Appl. Opt.* **41**, 116–124 (2002).
29. E. Götzinger, M. Pircher, M. Sticker, A. F. Fercher, and C. K. Hitzenberger, "Measurement and imaging of birefringent properties of the human cornea with phase-resolved, polarization-sensitive optical coherence tomography," *J. Biomed. Opt.* **9**, 94–102 (2004).
30. R. Angeles, T. Abunto, C. Bowd, L. M. Zangwill, D. Schanzlin, and R. N. Weinreb, "Corneal changes after laser *in situ* keratomileusis: measurement of corneal polarization magnitude and axis," *Am. J. Ophthalmol.* **137**, 697–703 (2004).
31. E. Götzinger, M. Pircher, M. Sticker, I. Dejaco-Rushwurm, S. Kaminski, C. Skorpik, A. F. Fercher, and C. K. Hitzenberger, "Pathologic changes of corneal birefringence imaged with polarization-sensitive optical coherence tomography," *Annual Meeting Abstract and Program Planner* accessed at [www.arvo.org](http://www.arvo.org), Association for the Research in Vision and Ophthalmology, Abstract 3668 (2003).
32. G. J. van Blokland and S. C. Verhelst, "Corneal polarization in the living human eye explained with a biaxial model," *J. Opt. Soc. Am. A* **4**, 82–90 (1987).